Bull. Chem. Soc. Ethiop. **2026**, 40(12), 2503-2521. ISSN 1011-3924
© 2026 Chemical Society of Ethiopia and The Authors Printed in Ethiopia
DOI: https://dx.doi.org/10.4314/bcse.v40i12.1 Online ISSN 1726-801X

VALORIZATION OF COOKED RICE WASTE VIA ACTIVATED CARBON SYNTHESIS AND APPLICATION IN REMOVAL OF METHYL ORANGE DYE FROM WATER

Nasser F. Alotaibi

Chemistry Department, College of Science, Jouf University, Sakaka, Saudia Arabia

(Received September 27, 2025; Revised February 19, 2026; Accepted March 4, 2026)

ABSTRACT. This study explores the conversion of cooked rice waste (CRW) into an affordable, activated carbon material with effective adsorption capabilities. Activated carbon (AC) was initially produced through combustion under a nitrogen atmosphere at 550 ℃. The resulting charcoal was then chemically activated using phosphoric acid (H_3PO_4). The FT-IR, XRD, SEM, and TGA techniques were used to characterize the produced AC. The characterization analysis showed that the AC has an amorphous surface with varied pore sizes, and that CRW was richer in functional groups than the prepared activated carbon. The obtained AC demonstrates effective adsorption capabilities for removing methyl orange dye (MO), achieving a maximum adsorption capacity of 3.68 mg/g at 298 K over a 30 min contact period. Regression coefficients indicated that the adsorption behavior followed the Freundlich isotherm model and pseudo-second-order kinetics. Response surface methodology (RSM) confirmed that the predicted results were in significant agreement with experimental results.

KEY WORDS: Water treatment, Methyl orange, Activated carbon, Cooked rice waste

INTRODUCTION

The increasing production of food waste poses a major global challenge with significant economic, environmental, and social implications [1]. Approximately 2.5 billion tons of food are wasted annually worldwide according to the Food and Agriculture Organization of the United Nations (FAO) [2, 3]. For instance, 133 billion pounds of food are wasted in the United States alone, amounting to $161 billion. This figure is equivalent to 31% of the total food supply and 25% of all municipal solid waste [4]. In Saudi Arabia, 4,066,000 tons of food waste are produced each year. Over 18% of the Kingdom's entire food supply is wasted, and the annual monetary value of food waste in the consumer expenditure category exceeds $11 billion per year [5, 6]. Food waste refers to any food that is generated at any stage within the food chain and not consumed by humans [2]. The food waste can be divided into raw and cooked food waste. According to the U.S. Environmental Protection Agency, the five sectors that generate food waste are institutional, commercial, industrial, residential, and waste from food banks. Offices, hospitals, jails and prisons, nursing homes, and universities all produce institutional garbage. Similarly, restaurants, motels, supermarkets, and other food vendors generate commercial trash [7].

Recently, efforts have been made to redirect food waste from landfills through recycling processes. Consequently, numerous reports and research papers have been published on the recycling of raw food waste, such as eggshells, agricultural waste, and other materials [8, 9]. However, few studies have been published about cooked food waste, which can be treated and used as an activated carbon (AC) precursor [2, 3].

The activated carbon has been demanded extensively due to its ability to work as an effective adsorbent for many pollutants. The most common precursor for activated carbon is the organic materials, such as food waste, due to their richness in carbon [10]. To produce AC by the chemical

*Corresponding author. E-mail: nfalotaibi@ju.edu.sa
This work is licensed under the Creative Commons Attribution 4.0 International License

activation technique, several chemical activating agents have been used [11], including H_2SO_4 and KCl [12], H_3PO_4[13], KOH[14], Na_2CO_3[15], and $ZnCl_2$ [16]. These substances have a major effect on the surface area, porosity, and active sites of AC during the synthesis process. The best choice for activating AC is phosphoric acid (H_3PO_4) due to its cost-effectiveness and environmental advantages, as well as the variety of micropores and mesopores it produces [17, 18].

One of the common pollutant dyes used in the textile industry is methyl orange (MO) [19, 20]. Unfortunately, it contributes to the pollution of the environment as it is consumed in high quantities in the wet process of textile coloring. A number of techniques can be used to remove MO dye from water, such as photocatalytic degradation [21, 22], electrochemical degradation [23, 24], and advanced oxidation processes [25]. However, the adsorption technique is preferred over other techniques due to its simplicity in operation and design, low cost of operation, and low toxicity [26, 27].

The recycling of food waste to synthesize activated carbon has been performed by many researchers. For example, coffee grounds were used as a precursor for AC to adsorb MO dye from an aqueous medium. The published results showed that the adsorption process followed the Freundlich model and had a capacity of 658 mg/g [28]. Moreover, cooked food waste was used as a precursor for activated carbon [2]. After activation with NaOH and KOH, it was used to remove methylene blue dye and acetic acid from an aqueous solution. It showed a low capacity of adsorption, which was 1.83×10^{-3} and $1.95x10^{-3}$ mg/g for acetic acid and methylene blue, respectively. The adsorption followed the Freundlich model and the pseudo-second order model [2].

Hence, the goal of this study is to convert food waste, namely, cooked rice waste, to yield AC using H_3PO_4 activation. The choice of rice as a precursor for AC preparation is because it is one of the most significant and extensively used cereal crops in Saudi Arabian diets, with an average annual consumption rate of 40 kilograms per person [29]. This promising, low-cost AC will be applied to remove MO dye from water via adsorption. The synthesized adsorbent will be evaluated by studying several factors, including dye concentration, pH, and contact time.

EXPERIMENTAL

Materials

Every chemical used in this study, such as phosphoric acid (98%, Sigma-Aldrich), sodium dodecyl sulfate (SDS), and methyl orange (MO), was bought from Sigma Aldrich and used without further purification.

Synthesis of activated carbon

The CRW was collected from a restaurant in the local area of Sakakah city, Al-Jouf province in KSA. Then, it was washed with surfactant (1% w/v SDS) to remove any residue of cooking oil or other contaminant. It was dried at 65 ^{o}C for 24 hours by using an oven after washing step with deionized water. Muffle at 550 ^{o}C for 2 hours under nitrogen gas was applied to carbonize the dried rice. The resulting material was crunched and activated using impregnation method in 85% phosphoric acid in the ratio of 1:4 w/v for 24 hours at room temperature [30, 31]. After that, the residue acid was washed several times till filtrate was neutral. The prepared AC was dried in oven at 65 ^{o}C for 24 hours than stored in closed container.

Sample characterization

The following instruments were used to physically characterize the raw material and final AC product: The Fourier transform FT-IR infrared spectrometer for functional group analysis (Shimadzu IR Tracer-100, Japan); X-ray diffractometer with 2θ in the 10°–80° range (Shimadzu XRD-7000, Japan) for phase analysis and crystallographic investigations, SEM(Quattro S - Thermo Scientific, USA) for surface morphology analysis; TGA analysis (TGA-51 Shimadzu thermogravimetric analyzer (Japan)) for thermal stability analysis; the UV-Vis spectrophotometer (LABOMED spectrometer) in the 400-700 nm region.

Adsorption experiments

The investigation of the sorption abilities of AC toward MO was conducted using the following method: the samples of the produced AC in the same amounts of 0.2 g were added to 50 mL of the MO aqueous solutions with initial concentrations ranging from 1 to 14 mgL^{-1}. To achieve the equilibrium condition, the mixtures were magnetically agitated for 30 minutes with a mixing speed of 300 rpm (VELP scientifica) at room temperature. To extract the AC particles from the analytes, centrifuging was used for five minutes at 5000 rpm for 5 min (Frontier 5000 Multi-Pro series). Using the previously created calibration curve, the determination of MO concentration was obtained using a UV-Vis spectrophotometer by measuring the absorbance of the solution both before and after adsorption experiments at a wavelength of 465 nm.
The adsorption of methyl orange (MO) dye was calculated following the equation:

$$\%\ Adsorption = \frac{(C_0 - C_t)}{C_0} x\ 100 \quad (1)$$

Adsorption capacity was calculated at any time (t) via equation number (2) :

$$q_t = \frac{(C_0 - C_t)}{m} V \quad (2)$$

Where C_0 and C_t are the starting concentration and concentration after adsorption of MO, respectively, m is the adsorbent quantity (g) and V is the volume of solution in liters.

RESULTS AND DISCUSSION

Materials characterization

FT-IR

The characterization of functional groups in both disposed cooked rice and prepared AC was obtained in the region 400-4000 cm^{-1}. As seen in Figure 1, there is a comparison between disposed cooked rice as biomass material (A) and its AC (B). It can be noticed that the biomass was richer in functional groups than AC. The biomass material showed a band at 3294 $cm^{-1,}$ which can be attributed to N-H stretching and OH group[11]. Aliphatic C-H stretching and C=O stretching are the root causes of the bands at 2924 cm^{-1} and 1651 cm^{-1}, respectively. Ether and ester groups appeared at 1150 cm^{-1} and 1080 cm^{-1} due to C-O stretching. Appearance of band at 995 cm^{-1} was attributed to =C-O-C stretching [28, 32].

The activated carbon spectra showed alteration in peaks profile. The broad band at 3294 cm^{-1} disappeared during the carbonization process, and a small band appeared at 3500 cm^{-1}, which can be caused by moisture. The appearance of aliphatic stretching peaks at 2924 cm^{-1} and 2780 cm^{-1} indicated an amorphous carbon that was not totally converted to the C=C bond. Bands at

1735 cm^{-1}, 1643 cm^{-1}, and 1464 cm^{-1} were assigned to C=O stretching, C=C stretching, and C-H bending, respectively. The band at 1110 cm^{-1} was attributed to C-O stretching [32, 33].

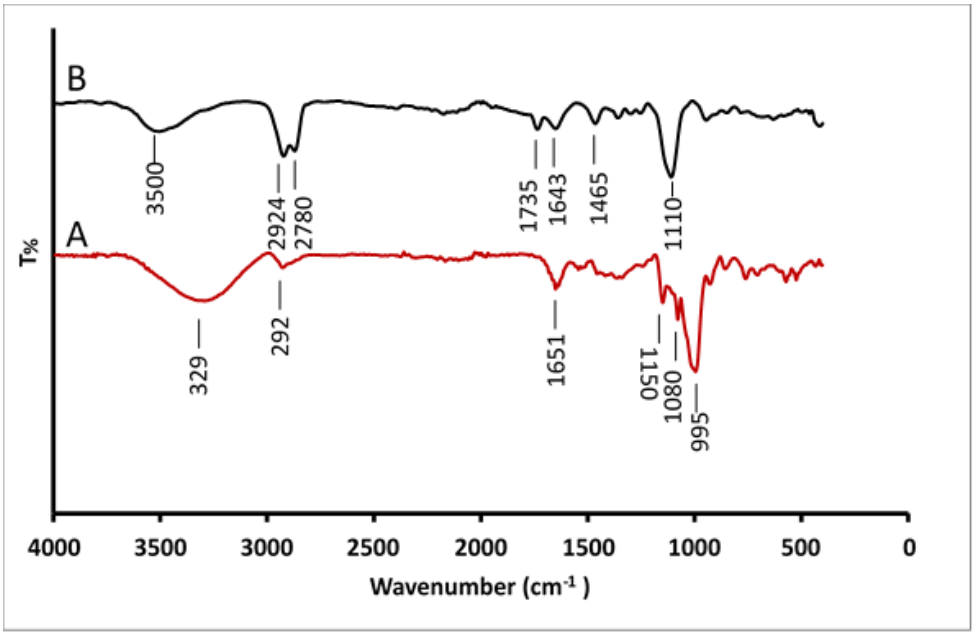

Figure 1. FT-IR spectra of (A) washed disposed rice and (B) activated carbon.

X-ray photoelectron spectroscopy (XPS)

In order to reveal the chemical composition of the synthesized AC, the XPS was utilized. The XPS survey spectrum (Figure 2a) showed characteristic peaks at 285.96, 534.33, and 400.93 eV, which were assigned to carbon, oxygen, and nitrogen, respectively. The phosphorus peak should appear at 131 eV, but it was not observed [3]. The percentages of carbon, oxygen, and nitrogen were 76.3%, 87.6%, and 2.1%, respectively. The residue percent was 2.96% can be accounted as ash materials [4].

XRD

Further structural investigation of the produced AC was obtained by powder XRD. Figure 2b showed the amorphous structure of AC. There were bands at 20°-30º and 40°-50º at reflection (002) and (100), which can be attributed to stacks of graphite layers. Therefore, the prepared carbon can be identified as carbon with an amorphous structure[32]. The average crystallite size (D) of AC was computed via apply the Scherrer equation. This is performed by focusing on the strongest peaks in the XRD patterns.

$$D = k\lambda/\beta\cos\theta \quad (3)$$

According to the Scherrer equation, λ indicates the radiation wavelength, k represents the form factor, while β is the full width at half maximum (FWHM in radians). The estimated crystallite sizes are 1.14 nm.

XRD reveals that the crystallite of AC was 12.4% while the amorphous percentage was 87.6%. This value is in the range of other literatures which used different organic materials [34, 35].

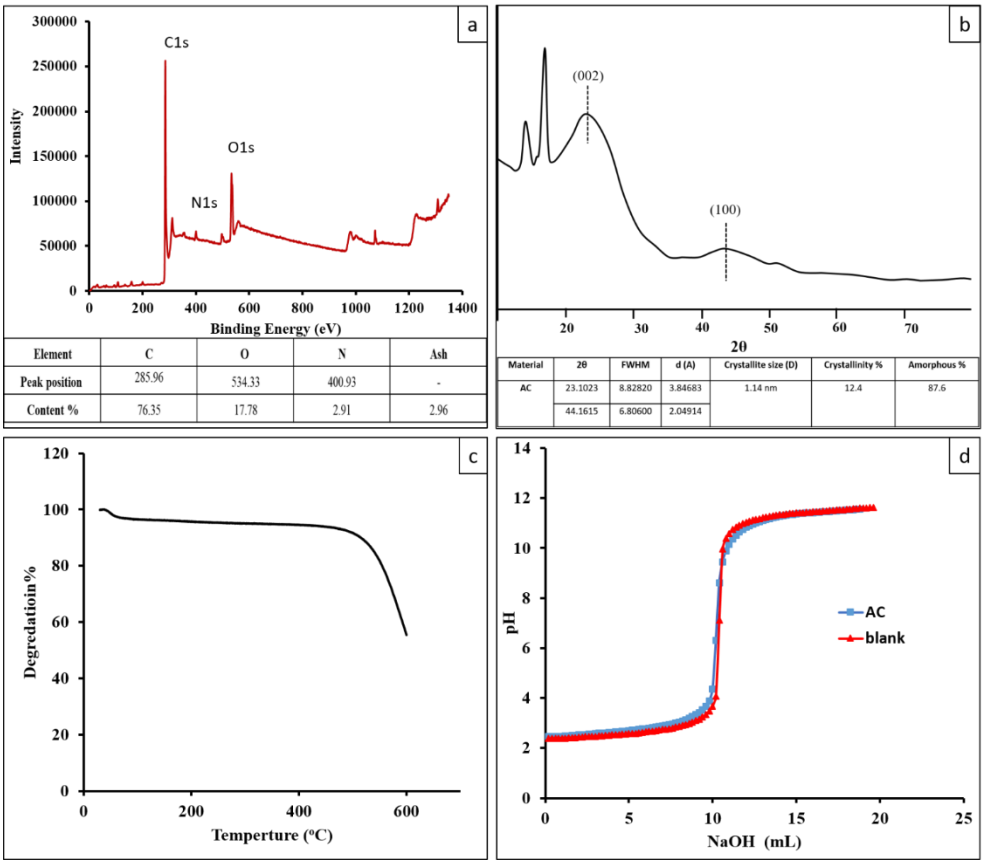

Element	C	O	N	Ash
Peak position	285.96	534.33	400.93	-
Content %	76.35	17.78	2.91	2.96

Material	2θ	FWHM	d (A)	Crystallite size (D)	Crystallinity %	Amorphous %
AC	23.1023	8.82820	3.84683	1.14 nm	12.4	87.6
	44.1615	6.80600	2.04914			

Figure 2. XPS result of prepared activated carbon revealing peak of main component (a), XRD pattern of prepared activated carbon showing amorphous structure (b), and TGA curve of activated carbon in air atmosphere within the range from 25 to 600 °C (c), and pH titration using potentiometric titration (d).

TGA

Thermal degradation of the produced AC was performed as shown in Figure 2c. The results of AC degradation in air were recorded in the heating range from 25 to 600 °C. The prepared AC showed high stability in the range from 25 to 450 °C, except for a slight change before 100 °C, which was due to the evaporation of moisture. At temperatures higher than 450 °C, gradual degradation was observed till 600 °C [32, 36].

BET analysis

Evaluation of the specific surface area was obtained by using an automated adsorption apparatus (Quantachrome, ASiQwin, version 3.01) through N2 adsorption– desorption analysis at 77.350 K. The BET equation was utilized to evaluate the nitrobrnt isotherms. Quenched solid density functional theory (QSDFT) was applied to nitrogen gas adsorption to evaluate the distribution of the pore size via the slit-shaped pores [32].

Surface area influences the adsorption process. Therefore, BET analysis was performed, and the result revealed that the surface area, pore volume, and pore radius were 41.863 m^2/g, 0.030 cc/g, and 7.122 Å, respectively. The surface area of AC affects the efficiency and capacity of the adsorption process, as seen in Figure 4 [37]. The surface area value was in the same range as previous work, which had surface area of 40.21 m^2/g [32].

SEM

Surface morphology of the adsorbent must be investigated due to its influence on the adsorption process. Figure 3 shows the morphology of the pore structure of the prepared AC. Pores of different sizes can be observed on the surface of AC (Figure 3A and 3C). The nature of raw materials, the manner of perpetration and the activation method can all have an impact on the production of micropores, mesopores, and macropores [38]. Figure 3D showed amorphous carbon on the surface, which confirmed the XRD results.

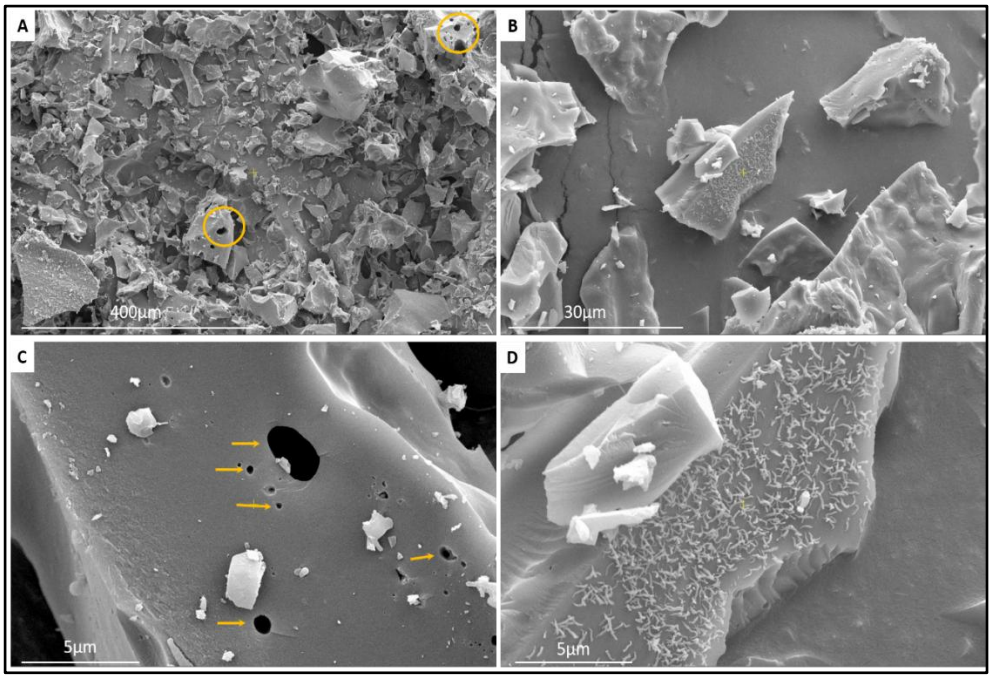

Figure 3. SEM images of prepared activated carbon showing pores on surface.

Adsorption studies

Determination of the point of zero charge (PZC)

PZC was determined via potentiometric titrations as reported [39]. The electrolyte ($NaNO_3$) solution with 0.1 M concentration and 40 mL was mixed with 0.1 g of the AC sample and stirred for 50 min to reach the equilibrium at room temperature. An addition of 2 mL of nitric acid (HNO_3) with a 0.1 M concentration was added with continuous stirring for 20 min. The pH values of the mixture were recorded using a pH meter. The titration was performed by the addition of 0.2 mL of NaOH with a 0.05 M concentration. The mixture was equilibrated for 2 min before the

value was recorded. The end of titration can be obtained when the change in pH value is less than 0.01 pH units min^{-1}. The blank titration was obtained for the mixture without the AC sample.

As seen in Figure 2d, the titration curve showed an intercept of the AC titration curve with the blank titration curve at pH 9. The surface charge of AC will be negative above PZC (pH 9), and the surface charge will be positive below pH 9.

Effect of pH

The adsorption process is affected by pH of the solution due to changes in the adsorbent's surface charge. Figure 4a shows the adsorption of MO dye onto the prepared activated carbon over a pH range of 2, 5, 7, 8 and 10 under conditions of room temperature, a 10 $mg \cdot L^{-1}$ dye concentration, and a 30 minute contact time. In general, adsorption decreases as the pH changes from acidic to basic. This agrees with published results [28] which reported that the adsorbent surface is negatively charged above pH 8 and positively charged below this value. The most efficient adsorption occurred at pH 2, with a gradual decrease at higher pH values. This is because the adsorbent surface has a positive charge in acidic media, which enhances the adsorption of the anionic MO dye. The basic medium led to a weak electrostatic interaction [33, 40].

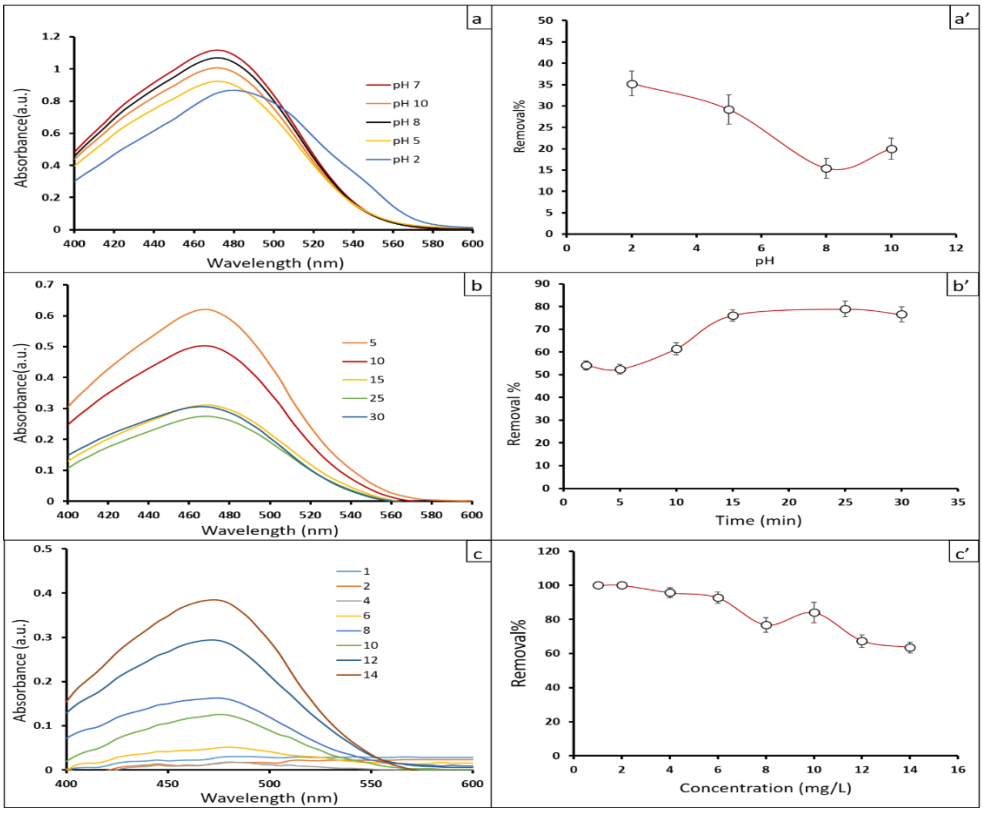

Figure 4. The effect of pH, contact time and concentration on adsorption of MO on adsorbent surface.

Effect of contact time

Contact time is one of the important factors in the adsorption process. Figure 4b illustrates the effect of contact time on the removal percentage. As shown in Figure 5b', the removal percentage increases with longer contact time and reaches equilibrium after 15 minutes. For contact times less than 15 minutes, the adsorption rate was fast due to the availability of active sites on the AC surface. After 15 minutes of contact time, the saturation of active sites and the slow pore diffusion of MO dye molecules from the solution to the surface occurred [28].

Effect of concentration

As illustrated in Figure 4c, the effect of MO concentration was investigated in the range (1, 2, 4, 6, 8, 10, 12, 14 mgL^{-1}) after 30 minutes contacting time and at room temperature. The removal of MO dye was completely obtained at a concentration of less than 10 mgL^{-1}. Then, the decrease in dye removal was observed as the concentration of dye increased. It is attributed to the decrease in active site vacancies at concentrations more than 8 mgL^{-1}.

Adsorption isotherm models

The adsorption isotherm models provide an explanation for the MO dye interaction on the surface of activated carbon. This search was conducted using the Temkin, Freundlich, Langmuir, and Dubinin Radushkevich (D-R) models [11]. All results were illustrated in Figure 5 and Table 1.

Langmuir model

The formation of a monolayer of adsorbate on the homogeneous surface of the adsorbent without interaction between dye molecules can be described using the Langmuir model. The linear form of Langmuir equation is illustrated as follows:

$$\frac{C_e}{q_e} = \frac{1}{q_0 K_L} + \frac{1}{q_0} C_e \tag{4}$$

Where q_e (mg/g) and C_e (mg/L) are the adsorption capacity and equilibrium concentration, K_L and q_o are the Langmuir constant and the adsorbent maximum monolayer capacity [41]. The correlation coefficient R^2 was 0.94, which indicates the adsorption occurred as monolayer molecules on a homogenous surface. The adsorption process occurrence can be confirmed by calculating the dimensionless equilibrium R_L as follows:

$$R_L = \frac{1}{1 + K_L C_0} \tag{5}$$

Where C_o is the maximum concentration of the investigated dye. The value of R_L indicates whether the process is unfavorable ($R_L > 1$), favorable ($0 < R_L < 1$), linear ($R_L = 1$), or irreversible ($R_L = 0$) [41]. The calculated value of R_L was 0.0037, which indicates a favorable process.

Freundlich model

Formation of multilayer coverage of dye molecules on the heterogeneous surface of the adsorbent can be expressed using the Freundlich model. The following equation is a representation of the Freundlich equation in its linear form:

$$\ln q_e = \ln K_F + \frac{1}{n} \ln C_e \tag{6}$$

Where the Freundlich constants are K_F and n [33]. The obtained R^2 value of 0.97 was higher than that of the Langmuir model, indicating that the adsorption process follows the Freundlich model more closely than the Langmuir model. This finding is in good agreement with the SEM images (Figure 3) and the XRD results (Figure 2b). The SEM images show a heterogeneous surface with varied pore sizes, which supports the assumption of the Freundlich model.

Temkin model

This model assumes that the interaction between adsorbate and adsorbent causes a decrease in adsorption heat (ΔH) of all molecules. It is expressed as follows:

$$q_e = B \ln K_t + B \ln C_e \tag{7}$$

Where K_t and B are the Temkin constant and the binding constant. The positive or negative value of B constant indicates whether the adsorption is exothermic or endothermic [28]. As seen in Table 1, the B value is a positive indication of an endothermic process.

Dubinin-Radushkevich model

The understanding of the bonding type between adsorbate and adsorbent, whether physical or chemical, can be described via the Dubinin-Radushkevich model. Its equation can be presented as follow [42]:

$$\ln q_e = \ln q_m - \beta\varepsilon^2 \tag{8}$$

Where β and ε are constants related to free energy and Polanyi potential can be expressed as follows:

$$\varepsilon = RT \ln\ (1 + {}^{1}/_{C_e}) \tag{9}$$

Adsorption mean free energy was calculated according to equation:

$$E = \frac{1}{\sqrt{(-2\beta)}} \tag{10}$$

The adsorption process mechanism is described by the value of E. The adsorption is physical when the value is less than 8 kJ/mol and will be chemical if the value is between 20 and 40 kJ/mol. The calculated E value was 7.9 kJ/mol, which was described as chemical adsorption [42].

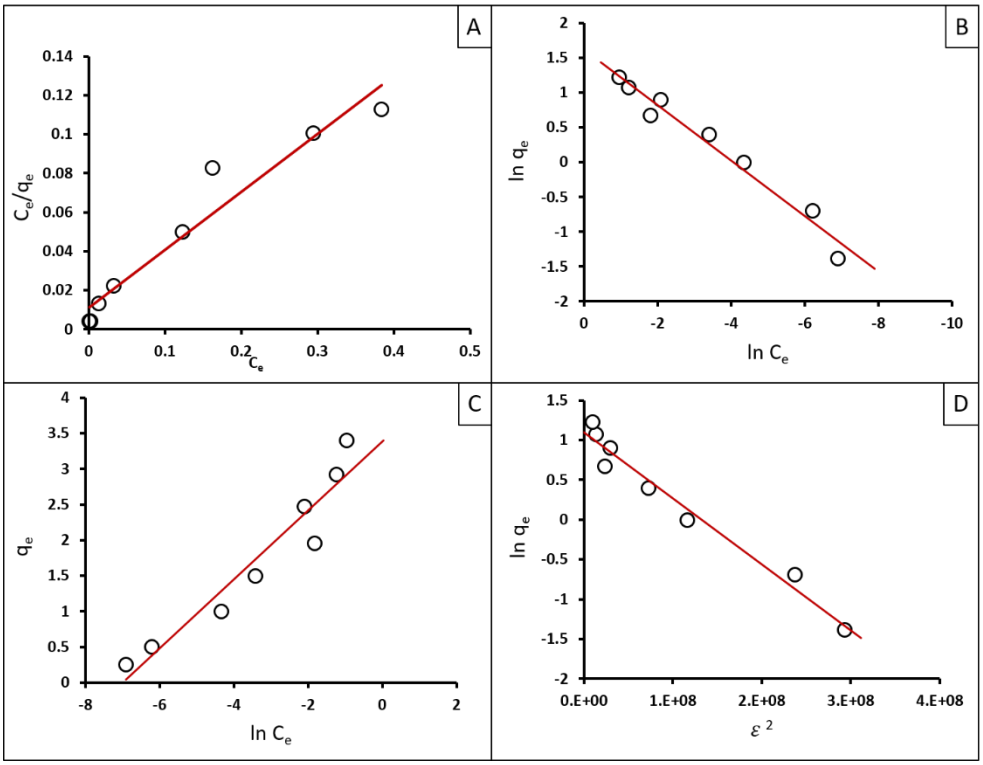

Figure 5. The plots of different isotherm models: (A) Langmuir model, (B) Freundlich model, (C) Temkin model, (D) Dubinin Radushkevich model.

Table 1. Calculation results of isotherm parameters of adsorption process of MO on activated carbon surface.

Model	Equation	Parameters	value
Langmuir	$\frac{C_e}{q_e} = \frac{1}{q_0 K_L} + \frac{1}{q_0} C_e$	q_o	3.368
		K_L	26.75
		R_L	0.0037
		R^2	0.94
Freundlich	$\ln q_e = \ln K_F + \frac{1}{n} \ln C_e$	K_F	5
		n	2.5
		R^2	0.97
Temkin	$q_e = B \ln K_T + B \ln C_e$	B	0.4822
		K_T	1097
		R^2	0.91
Dubinin Radushkevich (D-R) Isotherm	$\ln q_e = \ln q_m - \beta \varepsilon^2$	β	-8×10^{-9}
		q_m	3
		E	7.9 kJ/mol
		R^2	0.97

Kinetics of adsorption process

The adsorption kinetic behavior of MO dye on AC was studied using five models: first-order, pseudo-first-order, second-order, pseudo-second-order, and intraparticle diffusion. The linear

form of these models was used, and the regression coefficient (R^2) value indicated the best-fitting model. All results are illustrated in Figures 6 and Table S3 [43].

First-order model

The following is an expression for the equation of the first-order model:

$$ln\ C_t - lnC_o = -kt \tag{11}$$

As seen in Figure 6A, the correlation coefficient value (R^2) is 0.81which indicating to low value [44].

Second-order model

A linear equation of the second order model can be expressed as follows:

$$\frac{1}{C_t} - \frac{1}{C_o} = kt \tag{12}$$

As seen in Figure 6B, the plotting of $1/C_t$ against t was used to calculate the correlation coefficient value (R^2 = 0.81), which was not satisfied value[44].

Pseudo first model

This model may be expressed in the following linear form:

$$\ln(q_e - q_t) = \ln q_e - k_1\, t \tag{13}$$

Figure 7C shows the plotting of ln (q_e – q_t) versus t. It was employed to determine k_1 and q_e values [32]. The correlation coefficient (R^2) value was 0.81, which indicates a low value.

Pseudo-second model

This model assumes that chemisorption is occurring on the surface as the rate-determining step. The following equation is the linear form:

$$\frac{t}{q_t} = \frac{1}{k_2 {q_e}^2} + \frac{t}{q_e} \tag{14}$$

Plotting t/q_t against t, as shown in Figure 6D, was applied to calculate k_2 and q_e[32]. The correlation coefficient (R^2) value was 0.999, representing the best fitting model, which describes the behavior of MO dye on the activated carbon surface. As seen in Table 2, the experimental and calculated capacities were 2.43 mg/g and 2.44 mg/g, respectively. It presented good agreement.

Intra-particle diffusion model

The mechanism of dye adsorption is described by this model. It assumes that the diffusion of the adsorbate molecule into the interior of the adsorbent pores and the formation of binding is the rate-determining step [45].

It is expressed by the following equation:

$$q_t = k_i t^{1/2} + C \tag{15}$$

Where k_i and C are the diffusion rate constant and boundary layer thickness. Figure 6F showed the plot of q_t against $t^{1/2}$.

It is necessary for the plot's straight line to pass through the origin. Otherwise, the intercept sheds light on film diffusion. The diffusion process has three stages. First, move the dye molecules to the AC's outside surface. Transporting molecules into the AC's pores is the second stage. Finally, the adsorption of molecules on the interior surface of AC [32].

As seen in Table S3, the boundary layer thickness (intercept) value is 1.5, and the R^2 value is 0.97. It indicates that the adsorption process did not depend on the intraparticle diffusion step [45, 46].

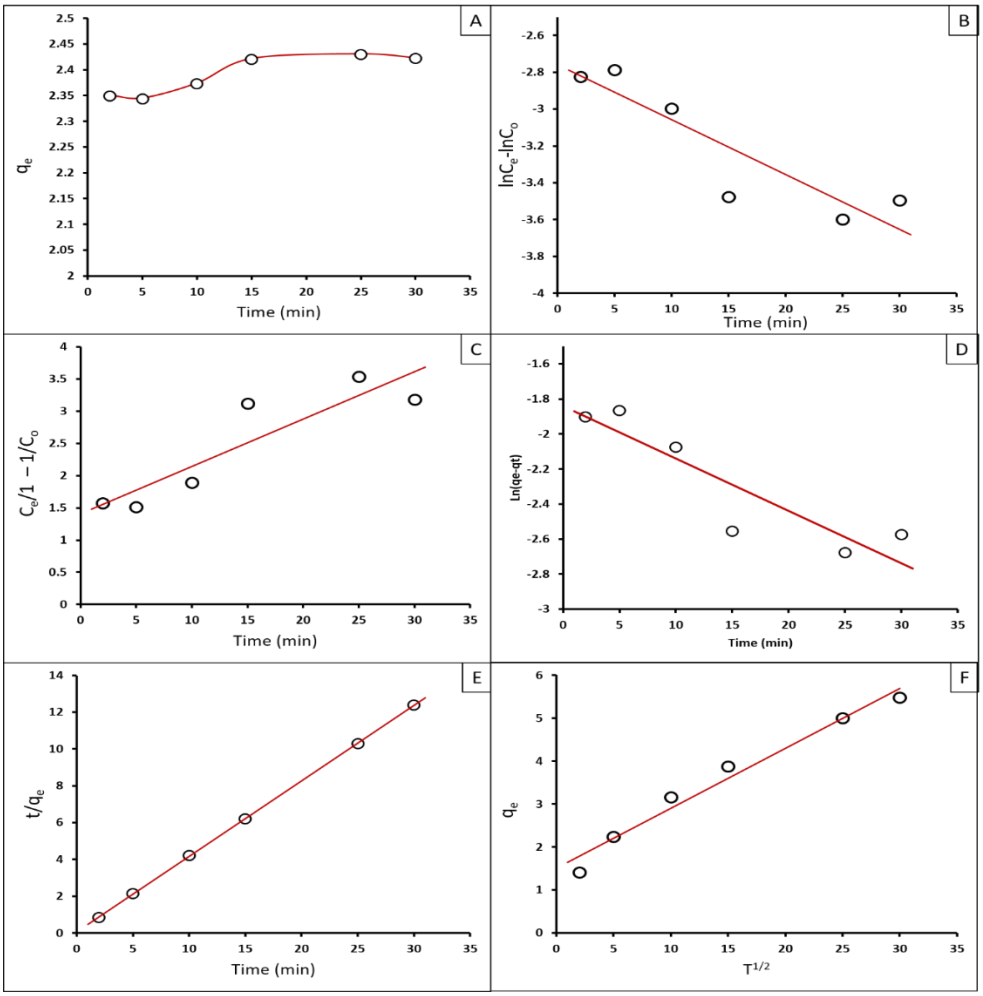

Figure 6. The kinetic models of adsorption: (A) impact of time on adsorption capacity, (B) first-order model, (C) second-order model, (D) pseudo-first model, (E) pseudo second model, (F) Intra-particle diffusion.

Mechanism of MO removal

The experimental data obtained would be useful to understand which steps control the overall removal rate of MO dye using the prepared AC. The adsorption of adsorbate on the AC surface

follows three steps: (i) transport of dye molecules to the external AC surface, (ii) diffusion of dye molecules within AC pores, (iii) adsorption of molecules on the exterior adsorbent surface. The final step happened quite quickly and isn't thought to be the one that determines the rate. According to the kinetic data, the adsorption process was independent of the intra-particle diffusion stage.

Adsorption of mixture dyes

The ability of synthesized activated carbon (AC) was examined by the mixture of methyl orange (MO) as an anionic dye and rhodamine B (RhB) as a cationic dye. The study was performed at pH 2 due to high removal efficiency as seen in the effect of pH section. Dye concentration was 10 mgL^{-1} for both in 50 mL at room temperature in one beaker. The mixture of dyes was mixed with 0.2 g of AC for at least 30 min at pH 2. Due to the color change of MO at pH 2 and the spectrum shift, pH was adjusted to be neutral to overcome the interface of the two dye spectra. Figure 7a shows the spectrum of the mixture of dyes before and after the adsorption process. It was observed that both dyes were adsorbed, showing a decrease in absorbance. Therefore, AC can be used as a nonselective adsorbent.

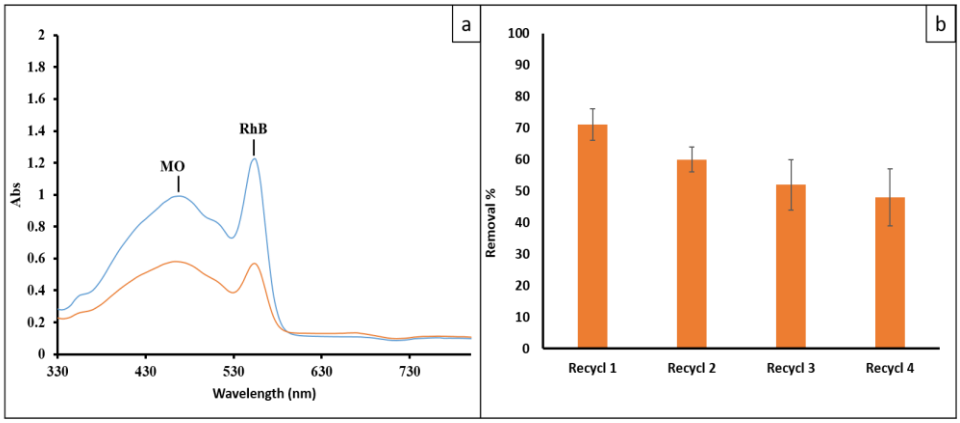

Figure 7. Spectrum of mixture of MO and RhB dyes (a), recyclability of AC adsorption for four times (b).

Recyclability investigation of the adsorbent

The investigation of the recyclability of AC is one of the crucial methods that evaluates the durability of adsorbent usage. The MO removal percentage for four times recycling was recorded over time of reuse as displayed in Figure 7b. After each cycle, AC was washed with 10 mL of methanol three times till the solution became colorless. After that, the AC was heated in the oven at 75 °C for 2 hours. The separation of AC from the solution was performed by using centrifuging at 6000 rmp for 3 min. The recycling was performed at pH 2, 10 mg/L concentration, 0.2 g AC dose, and 50 mL solution volume. The average removal percentage was 71% of the first cycle, and it decreased until the removal reached about 48% after four cycles.

Response surface methodology (RSM)

The optimization of three independent variables takes a number of trials, which consumes time, effort, and materials. Response surface methodology (RSM) can be used to minimize the overall

costs to obtain the best condition to achieve sufficient results. In this work, a central composite design (CCD) was used to specify the optimal conditions for illumination of MO dye from water. The approach was carried out by keeping all variables constant and varying one factor at a time. It helped to minimize the range of concentration, pH, and contacting time. The response prediction equation (qt) was obtained as follows:
With coded factors**:**

$$qt = 2.18 + 0.6778A - 0.0373B - 0.2031AB - 0.3249A2 + 0.0824B2 \quad (16)$$

With actual factors:

$$qt = 0.8486 + 0.2553A + 0.000627B - 0.002232AB - 0.007689A2 + 0.000420B2 \quad (17)$$

This equation can be used to estimate the value of qt for any concentration and contact time level within the study limits.

As seen in Table S1 in the supplementary section, ANOVA results depict that the promoted model has a high F-value (20.67) and a low p-value (0.0005), which indicate that the model is statistically significant for fitting experimental data [47]. In table S2, the value of R^2 (0.9753) was indicating to fit of a quadratic model to the experimental data. It indicates that the results of the experiment and the predictions agreed rather well [48]. Figure S1 shows the experimental design matrix and the ability of dye removal when the AC was utilized as an adsorbent, showcasing both expected and experimental outcomes. In Figure 8, the examination of operational parameters (concentration, pH, and contact time) was done to ascertain the impact of these variables on the removal of MO dye. The determining factor was concentration as it relates to the availability of adsorption sites on the AC surface. Moreover, other factors such as electrostatic attraction and surface morphology may influence dye adsorption at different pH levels. The experimental results of the qt values were aligned with the RSM results. Figure S2 shows the optimum values of the parameters (concentration, pH, and contact time) for achieving maximum performance using AC to remove MO dye.

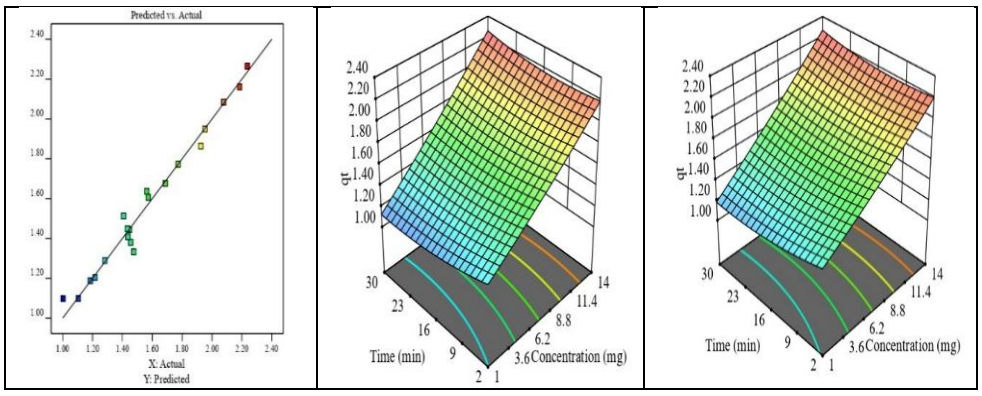

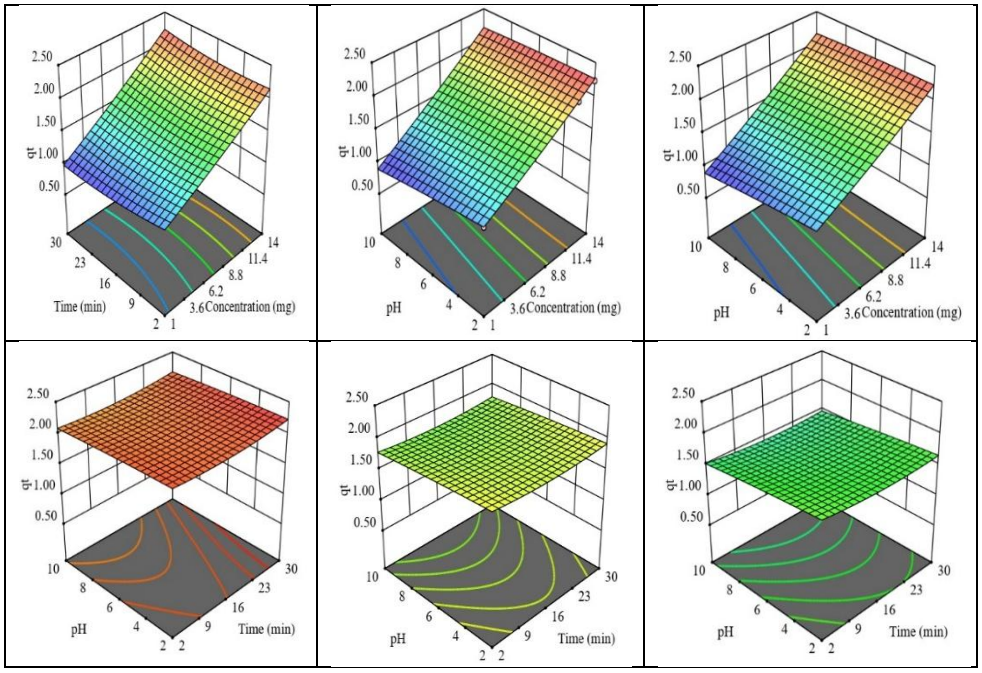

Figure 8. Model-predicted versus experimental values of MO (predicted vs. actual), and 3D response surface plots the effect of concentration, pH, and time on MO dye removal using AC.

Adsorption comparison and evaluation

To evaluate the current work and draw clear insights into the future work, a comparison of the MO dye's adsorption behavior on various adsorbent surfaces was done. Table 3 shows the data on different precursors of activated carbon. In terms of the kinetic model, the adsorption process follows the pseudo-second model of all the presented works. Langmuir was the isotherm model that assumes a monolayer of adsorbate covers the adsorbent particle surface. There was a variety in adsorption capacity, which can be attributed to the nature of the precursor and the activation process.

Table 3. Comparison between different biomass as activated carbon precursor used as adsorbent of methyl orang dye (MO).

Adsorbent precursor	Activation	Removal%	q	Kinetic model	Isotherm model	Ref.
Cooked rice	H_3PO_4	81	3.68	Pseudo-second	Freundlich	Current study
Peanut shell and rice husk	-	-	3.9-17.2	Pseudo-second	-	[49]
Date stones	KOH	76.6	56	Pseudo-second	Freundlich	[41]
Prickly pear seed cak	H_3PO_4	100	260	Pseudo-second	Freundlich	[50]
corncob	H_3PO_4	-	107.5	Pseudo-second	Langmuir	[51]
Wood sawdust	H_3PO_4	95	31.93	Pseudo-second	Langmuir	[46]
Activated charcoal	KOH	82	188.7	Pseudo-second	Langmuir	[52]

CONCLUSION

Activated carbon (AC) was synthesized from waste cooked rice as a precursor under a nitrogen atmosphere at 550 °C. The product was activated with phosphoric acid (H_3PO_4) and subsequently used to remove methyl orange dye (MO) from water via adsorption. The produced activated carbon was characterized using FT-IR, XRD, TGA, and SEM. The analysis revealed an amorphous surface with varied pore sizes. The adsorption isotherm and kinetic models were investigated. The Freundlich isotherm model showed a higher R^2 value (0.97) than the Langmuir model ($R^2 = 0.94$). Similarly, kinetic modeling showed that the pseudo-second-order model provided a better fit, with an R^2 of 0.999, compared to the pseudo-first-order model. The adsorption capacity of the adsorbent was 3.68 mg/g. Finally, the current study was contextualized by a comparison with published data, indicating that the nature of the precursor and the activation process control the adsorption performance.

ACKNOWLEDGMENTS

For their assistance and support during the study, the author would like to thank every member of the Chemistry Department at Jouf University's College of Science. The author would like to especially thank Dr. M. F. Hasaneen for his support in RSM section.

Funding statement

This work was self-funded.

Conflict of interest

The author declares no competing interests.

Data availability

Data will be available on request.

REFERENCES

1. Yılmaz, S.; Günal, A. M.; Köse, G.; Baş, M. The Environmental and economic dynamics of food waste and greenhouse gas emissions: A causal time series analysis from 2000 to 2022. *Sustainability* **2025**, 17, 775.
2. Krithiga, T.; Sabina, X. J.; Rajesh, B.; Ilbeygi, H.; Shetty, A. N.; Reddy, R.; Karthikeyan, J. Cooked food waste—an efficient and less expensive precursor for the generation of activated carbon. *J. Nanosci. Nanotechnol.* **2018**, 18, 4106-4113.
3. Yin, Y.; Gong, H.; Chen, Z.; Tian, X.; Wang, Y.; Wang, Z. **;**He, K.; Miao, Q.; Chu, Y.; Xue, Y.; Zhang, Q.; Cui, Z. Underestimated sequestration of soil organic carbon in China. *Environ. Chem. Lett.* **2025**, 23, 373-379.
4. Vogliano, C.; Brown, K. The state of America's wasted food and opportunities to make a difference. *J. Acad. Nutr. Diet.* **2016**, 116, 1199-1207.
5. Alshabanat, Z.; Alkhorayef, A.; Ben Haddad, H.; Mezghani, I.; Gouider, A.; Tlili, A.; Allouche, M. A.; Gannouni, K. A. Quantifying food loss and waste in Saudi Arabia. *Sustainability* **2021**, 13, 9444.
6. Ahmed, A.E.; Alzahrani, F. Food loss and waste in Saudi Arabia: Analysis, Causes, and Interventions, in: A.E. Ahmed, J.M. Al-Khayri, A.A. Elbushra (Eds.), Food and Nutrition

Security in the Kingdom of Saudi Arabia, Vol. 2: Macroeconomic Policy and Its Implication on Food and Nutrition Security, Springer International Publishing, Cham, **2024**, 241-274.
7. Dou, Z.; Ferguson, J.D.; Galligan, D.T.; Kelly, A.M.; Finn, S.M.; Giegengack, R. Assessing U.S. food wastage and opportunities for reduction. *Glob. Food Sec.* **2016**, 8, 19-26.
8. Timur, S.; Kantarli, I.C.; Ikizoglu, E.; Yanik, J. Preparation of activated carbons from Oreganum stalks by chemical activation. *Energy Fuels* **2006**, 20, 2636-2641.
9. Hesas, R.H.; Arami-Niya, A.; Daud, W.M.A.W.; Sahu, J. Microwave-assisted production of activated carbons from oil palm shell in the presence of CO_2 or N_2 for CO_2 adsorption. *J. Ind. Eng. Chem.* **2015**, 24, 196-205.
10. Bulduk, İ.; Yilmaz, N.; Türk Baydir, A. Effective removal of cytotoxic cyclophosphamide from aqueous solutions using novel adsorbent (hemp root). *Bull. Chem. Soc. Ethiop.* **2025**, 39, 2329-2346.
11. Wang, F.; Qi, X.; Zhang, H.; Yang, Z. Innovative molten salt techniques for biomass valorization: Transforming biomass into advanced carbon materials. *Carbon* **2025**, 234, 119999.
12. Wong, S.; Yac'cob, N.A.N.; Ngadi, N.; Hassan, O.; Inuwa, I.M. From pollutant to solution of wastewater pollution: Synthesis of activated carbon from textile sludge for dye adsorption. *Chin. J. Chem. Eng.* **2018**, 26, 870-878
13. Sirajo, L.; Ahmad Zaini, M.A. Adsorption of water pollutants using H_3PO_4-activated lignocellulosic agricultural waste: A mini review. *Toxin Reviews* **2023**, 42, 349-361.
14. Genli, N.; Kutluay, S.; Baytar, O.; Şahin, Ö. Preparation and characterization of activated carbon from hydrochar by hydrothermal carbonization of chickpea stem: An application in methylene blue removal by RSM optimization. *Int. J. Phytoremediation* **2022**, 24, 88-100.
15. Uçar, S.; Erdem, M.; Tay, T.; Karagöz, S. Removal of lead(II) and nickel(II) ions from aqueous solution using activated carbon prepared from rapeseed oil cake by Na_2CO_3 activation. *Clean Technol. Environ. Policy* **2015**, 17, 747-756.
16. Al-Qaessi, F.A.H. Production of activated carbon from date stones by using zinc chloride. *Energy Sources A: Recovery Util. Environ. Eff.* **2010**, 32, 917-930.
17. Allbed, A.; Kumar, L.; Shabani, F. Climate change impacts on date palm cultivation in Saudi Arabia. *J. Agric. Sci.* **2017**, 155, 1203-2018.
18. Awang, H.F.; Jawad, A.H.; Annuar, N.H.R.; Alothman, Z.A.; Wilson, L.D. Converting blended chicken bone and rice food wastes into activated carbon via microwave process: Box-Benken optimization for methyl violet dye removal. *Water Air Soil Pollut.* **2024**, 235, 764.
19. Bazrafshan, E.; Zarei, A.A.; Nadi, H.; Zazouli, M.A. Adsorptive removal of methyl orange and reactive red 198 dyes by moringa peregrina ash. *Indian J. Chem. Technol.* **2014**, 21, 105-113.
20. Mo, J.H.; Lee, Y.H.; Kim, J.; Jeong, J.Y.; Jegal, J. Treatment of dye aqueous solutions using nanofiltration polyamide composite membranes for the dye wastewater reuse. *Dyes Pigments* **2008**, 76, 429-434.
21. Adeel, M.; Saeed, M.; Khan, I.; Muneer, M.; Akram, N. Synthesis and characterization of Co–ZnO and evaluation of its photocatalytic activity for photodegradation of methyl orange. *ACS omega* **2021**, 6, 14261435.
22. Luo, J.; Zhou, X.; Ma, L.; Xu, X.; Wu, J.; Liang, H. Enhanced photodegradation activity of methyl orange over Ag_2CrO_4/SnS_2 composites under visible light irradiation. *Mater. Res. Bull.* **2016**, 77, 291-299.
23. Li, S.-H.; Zhao, Y.; Chu, J.; Li, W.-W.; Yu, H.-Q.; Liu, G. Electrochemical degradation of methyl orange on Pt–Bi/C nanostructured electrode by a square-wave potential method. *Electrochimica Acta* **2013**, 92, 93-101.
24. Islam, M.M.; Basu, S. Effect of morphology and pH on (photo) electrochemical degradation of methyl orange using TiO_2/Ti mesh photocathode under visible light. *J. Environ. Chem. Eng.* **2015**, 3, 2323-2330.

25. Haji, S.; Benstaali, B.; Al-Bastaki, N. Degradation of methyl orange by UV/H_2O_2 advanced oxidation process. *Chem. Eng. J.* **2011**, 168, 134-139.
26. Ince, M.; Ince, O.K. An overview of adsorption technique for heavy metal removal from water/wastewater: a critical review. *Int. J. Pure Appl. Sci.* **2017**, 3, 10-19.
27. Kyzas, G.Z.; Fu, J.; Matis, K.A. The change from past to future for adsorbent materials in treatment of dyeing wastewaters. *Materials* **2013**, 6, 5131-5158.
28. Rattanapan, S.; Srikram, J.; Kongsune, P. Adsorption of methyl orange on coffee grounds activated carbon. *Energy Procedia* **2017**, 138, 949-954.
29. Abd-Rabboh, H.S.M.; Fawy, K.F.; Hamdy, M.S.; Elbehairi, S.I.; Shati, A.A.; Alfaifi, M.Y.; Ibrahium, H.A.; Alamri, S.; Awwad, N.S. Valorization of rice husk and straw agriculture wastes of eastern Saudi Arabia: Production of bio-based silica, lignocellulose, and activated carbon. *Materials* **2022**, 15, 3746.
30. Mohamed, E.F.; El-Hashemy, M.A.; Abdel-Latif, N.M.; Shetaya, W.H. Production of sugarcane bagasse-based activated carbon for formaldehyde gas removal from potted plants exposure chamber. *J. Air Waste Manag. Assoc.* **2015**, 65, 1413-1420.
31. Luo, Y.; Li, D.; Chen, Y.; Sun, X.; Cao, Q.; Liu, X. The performance of phosphoric acid in the preparation of activated carbon-containing phosphorus species from rice husk residue. *J. Mater. Sci.* **2019**, 54, 5008-5021.
32. El-Hashemy, M.A.E.-S.; Alotaibi, N.F. Purification of benzene-laden air by static adsorption of benzene onto activated carbon prepared from Diplotaxis acris biomass. *Biomass Convers. Biorefin.* **2023**, 13, 1763-1777.
33. Ramutshatsha-Makhwedzha, D.; Mavhungu, A.; Moropeng, M. L.; Mbaya, R. Activated carbon derived from waste orange and lemon peels for the adsorption of methyl orange and methylene blue dyes from wastewater. *Heliyon* **2022**, 8, e09930.
34. Khalil, H.; Jawaid, M.; Firoozian, P.; Rashid, U.; Islam, A.; Akil, H.M. Activated carbon from various agricultural wastes by chemical activation with KOH: Preparation and characterization. *J. Biobased Mater. Bioenergy* **2013**, 7, 708-714.
35. Shamsuddin, M.; Yusoff, N.; Sulaiman, M. Synthesis and characterization of activated carbon produced from kenaf core fiber using H_3PO_4 activation. *Procedia Chem.* **2016**, 19, 558-565.
36. da Silva Medeiros, D.C.C.; Usman, M.; Chelme-Ayala, P.; Gamal El-Din, M. Biochar-enhanced removal of naphthenic acids from oil sands process water: Influence of feedstock and chemical activation. *Energy Environ. Sustain.* **2025**, 2, 10002**.**
37. Alotaibi, N.F.; Hakami, A.; Alanazi, A.H.; Alanazi, F.K.; El-Hashemy, M.A.E.-S.; Alrashdi, B.M.; Rawway, M.; Nassar, A. Harnessing wasted palm tree leaf and its silver oxide composite for efficient sustainable remediation of toxic aquatic pollutants. *ChemistrySelect* **2025**, 10, e04481.
38. Xu, Y.; Fan, Z.; Li, X.; Yang, S.; Wang, J.; Zheng, A.; Shu, R. Cooperative production of monophenolic chemicals and carbon adsorption materials from cascade pyrolysis of acid hydrolysis lignin. *Bioresour. Technol.* **2024**, 399, 130557.
39. Mustafa, S.; Dilara, B.; Nargis, K.; Naeem, A.; Shahida, P. Surface properties of the mixed oxides of iron and silica. *Colloids Surf. A Physicochem. Eng. Asp.* **2002**, 205, 273-282.
40. Li, N.; Zhu, F.; Wang, Z.; Wu, J.; Gao, Y.; Li, K.; Zhao, C.; Wang, X. Harnessing corn straw biochar: A breakthrough in eco-friendly Cu(II) wastewater treatment. *Waste Manag.* **2025**, 197, 25-34.
41. Mitra, S.; Tirthankar, M.; Kaparaju, P. Prediction of methyl orange removal by iron decorated activated carbon using an artificial neural network. *Environ. Technol.* **2021**, 42, 3288-3303.
42. Khan, T.A.; Chaudhry, S.A.; Ali, I. Equilibrium uptake, isotherm and kinetic studies of Cd(II) adsorption onto iron oxide activated red mud from aqueous solution. *J. Mol. Liq.* **2015**, 202, 165-175.

43. Abeyrathna, W.; Cooray, A.; Walpita, J., Removal of Rhodamine B and malachite green from aqueous solutions using cinnamon wood biochar, proceedings of international forestry and environment symposium, **2022**.
44. Petrucci, R.H.; Cunningham, C.M.; Moore, T.E. *General Chemistry*. Macmillan New York **1989**, 551-557.
45. Chaudhry, S.A.; Ahmed, M.; Siddiqui, S.I.; Ahmed, S. Fe(III)–Sn(IV) mixed binary oxide-coated sand preparation and its use for the removal of As(III) and As(V) from water: application of isotherm, kinetic and thermodynamics. *J. Mol. Liq.* **2016**, 224, 431-441.
46. Sayed, N.S.; Ahmed, A.S.; Abdallah, M.H.; Gouda, G.A. ZnO@ activated carbon derived from wood sawdust as adsorbent for removal of methyl red and methyl orange from aqueous solutions. *Sci. Rep.* **2024**, 14, 5384.
47. Deb, A.; Debnath, A.; Saha, B. Sono-assisted enhanced adsorption of eriochrome Black-T dye onto a novel polymeric nanocomposite: Kinetic, isotherm, and response surface methodology optimization. *J. Dispersion Sci. Technol.* **2021**, 42, 1579-1592.
48. Seaf Elnasr, T.A.; Al-Enezi, A.T.; Hussein, M.F.; Bielal, H.; Alhumaimess, M.S.; El-Ossaily, Y.A.; Hassan, H.M.A.; AlNahwa, L.H.M.; Aldawsari, A.M.; Alsohaimi, I.H. Sustainable biodiesel production from waste olive oil: Utilizing olive pulp-derived catalysts for environmental and economic benefits. *Sustain. Chem. Pharm.* **2024**, 37, 101426.
49. Dong, Y.; Liang, J.; Song, J.; Liu, C.; Ding, Z.; Wang, W.; Zhang, W. Preparation of biochar/iron mineral composites and their adsorption of methyl orange. *RSC Adv.* **2024**, 14, 33977-33986.
50. El Maguana, Y.; Elhadiri, N.; Bouchdoug, M.; Benchanaa, M.; Jaouad, A. Activated carbon from prickly pear seed cake: Optimization of preparation conditions using experimental design and its application in dye removal. *Int. J. Chem. Eng.* **2019**, 2019, 8621951.
51. Abollé, A.; Urbain, K.Y.; Ollo, K.; Tchonrontcha, K.Y.; Rodrigue, K.A. Adsorption of methyl orange on corncob activated carbon: Kinetic, equilibrium, and thermodynamic studies. *Earthline J. Chem. Sci.* **2022**, 8, 205-224.
52. Indujalekshmi, J.; Arsha, M.; Biju, V. KOH-mediated structural modification of activated charcoal by heat treatment for the efficient adsorption of organic dyes. *Appl. Surf. Sci. Adv.* **2024**, 19, 100566.